FOCUSING OF OPTICAL TRANSITION AND DIFFRACTION RADIATION BY A SPHERICAL TARGET

L.G. Sukhikh*, G.A. Naumenko, and A.P. Potylitsyn
Tomsk Polytechnic University, Tomsk, Russia
J. Urakawa and A.S. Aryshev
KEK, Tsukuba, Japan
S. Boogert and P.V. Karataev
John Adams Institute at Royal Holloway, University of London, Egham, UK

Abstract

For the first time the focusing effect of optical transition and diffraction radiation generated by electrons with the energy of 1.28 GeV has been observed experimentally. A comparison of angular distribution of detected radiation was made for flat and spherical targets. It was shown, that application of such targets allows increasing the spectral-angular density in the focus of the sphere without any additional optical devices.

INTRODUCTION

Transition (TR) and diffraction (DR) radiation are widely used for an electron beam diagnostics. In the experiment [1] the authors have demonstrated the measurements of the transverse size of an electron beam via optical TR (OTR) imaging technique with the resolution of order of 2 µm. In the experiment [2], the transverse beam size was measured using optical DR (ODR) with the accuracy of order of 14 µm. But the advantage of the ODR technique is related to a possibility to perform an almost noninvasive beam diagnostics. Besides it is also possible to measure longitudinal beam size using coherent TR or DR. Authors of the paper [3] have focused coherent TR generated by a bunch with length of ~1mm onto an electro-optic crystal (EOC) using an external optical device. Under CTR field EOC characteristics were changed. It allowed to measure the bunch duration by monitoring the polarization variation of a stable laser. Sensitivity of the Electro-optic technique might be improved by increasing the CTR photon density on the EOC.

Recently we proposed to use focused coherent diffraction radiation (CDR) for soft x-ray generation via inverse Thompson scattering process [4].

In applications mentioned above there is one serious problem – so called "pre-wave zone effect", which becomes significant when the distance between target and detector is shorter than $\gamma^2\lambda$ [5], where γ is the charged particle Lorentz-factor and λ is the DR wavelength. Because of this effect the angular distributions of TR and DR become broader and the spectral-angular radiation density decreases. Those two facts seriously complicate the use of TR and DR for different applications.

The electro-magnetic field of an ultra-relativistic particle can be considered as a set of plane waves (in other words the behavior of the virtual photons of the particle field is similar to the behavior of real photons). That is why some of the present paper authors proposed [6,7] to use paraboloidal targets for TR (DR) generation in order to focus TR (DR) on a detector.

* Leonidus_ii@mai.ru

EXPERIMENTAL SETUP

In order to verify this approach we carried out an experiment at KEK-ATF (Accelerator Test Facility). The experimental setup is shown in Figure. 1. It has been installed in the diagnostics section of the KEK-ATF extraction line [8]. The extracted beam parameters in the vicinity of the target chamber during the experiment are listed up in Table 1.

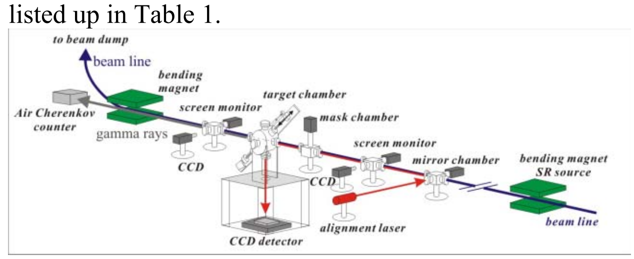

Figure.1 Experimental setup

Table 1. Beam parameters at the target chamber

Energy	1.28 GeV (γ=2500)
Bunch population	$0.9\cdot10^{10}$
Bunch repetition	1.56 Hz
Vertical beam size	σ_y=29.35±1.1 µm
Horizontal beam size	σ_x <150 µm

The target chamber has a very precise target stage actuator with linear movement accuracy better than 0.5 µm. The target chamber allows to install two targets. A 10µm thick tungsten wire was also installed in the target chamber, and the vertical beam size mentioned in the Table 1 has been measured using this wire. There was no possibility to measure the horizontal beam size in the target chamber directly. In the Table 1 the horizontal beam size was predicted by the SAD code [9].

The targets are very important parts of the experiment. Even a small deformation of target may cause a significant distortion of the ODR distribution. A flat target was a 300 µm thick gold-coated silicon wafer of 7×9 mm dimensions [2]. Instead of a paraboloidal target we used a spherical one. It is well-known that if the radiation spot dimension on the sphere surface is much smaller than its radius, the sphere can be approximated by a paraboloid. The spherical target was an aluminized glass segment with transverse dimension of 15×7.5 mm and 500 mm focus. Roughness of the target surfaces was less than 150 nm. Both targets were mounted in the target chamber with 45 deg to the beam trajectory. The targets installed allowed both OTR and ODR measurements. That is why the position of the target with respect to the electron beam is important. Measuring OTR one must be sure that there is no edge effect. Measuring ODR one should precisely know the impact-parameter (the shortest distance between the target edge and the electron trajectory). An air Cherenkov counter was used to measure the bremsstrahlung photons generated when the electron beam interacted with the target. The dependence of the detector response versus target position (see Figure. 2) allowed us to define the impact-parameter [8]. The air cherenkov signal dependence for single electron has a form shown by the dashed line in Figure.2. The point where this linear fit crossed abscissa is assumed to be the point of zero impact-parameter. Because of nearly Gaussian distribution of the electrons in vertical direction at the point of zero impact parameter half of the beam interacted with the target directly. The solid curve in the Figure.2 shows single electron dependence convoluted with Gaussian distribution (σ_V= 29 μm).

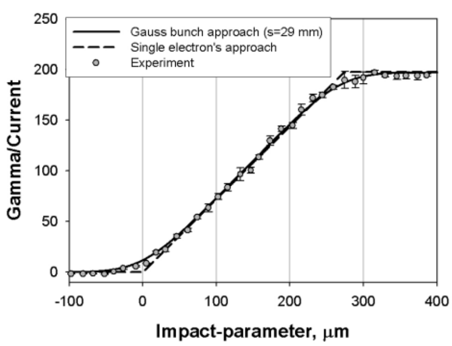

Figure 2. The dependence of air Cherenkov counter signal vs. impact-parameter (points); single electron approach (dashed line); Gauss bunch approach (solid line)

The optical system consisted of a polarizer, optical filter and highly sensitive cooled CCD-camera (Alta E4000). The main parameters of the CCD are listed-up in Table 2.

Table 2. CCD-camera characteristics

CCD	Kodak KAI-4020M
Pixel size (micron /γ^{1})	7.4×7.4 / 0.04×0.04
Imaging area (mm / pixels)	15.15×15.15 / 2048×2048
Quantum efficiency Peak (500 nm)	55%

The high quantum efficiency of the CCD-camera along with high bunch population allowed to carry out single-shot measurements.

The detector was installed at a distance of L=440 mm, which corresponds to 0.14 $\gamma^2\lambda$ (extreme pre-wave zone) for $\lambda = 500$ nm. A laser system consisting of a laser focusing system, a vacuum mirror, and two screen monitors was used for optical system alignment. The accuracy of this system was better than 0.4 mrad [8].

The ATF extraction line contains many different magnetic devices, which may lead to appearance of synchrotron radiation (SR) background. To avoid the SR contribution a mask has been installed half a meter upstream of the target to cut the SR off. The mask itself was a ceramic plate with a 1×2 mm hole in the center of it [10-11].

EXPERIMENTAL RESULTS

The OTR angular distributions of the vertical polarization component without optical filters from the both targets were measured. The theory predicted that for the experimental conditions OTR distribution from the spherical target would be almost two times narrower than from the flat one (the focusing effect). The measured distributions of OTR vertical polarization components of both targets are shown in Figure.3.

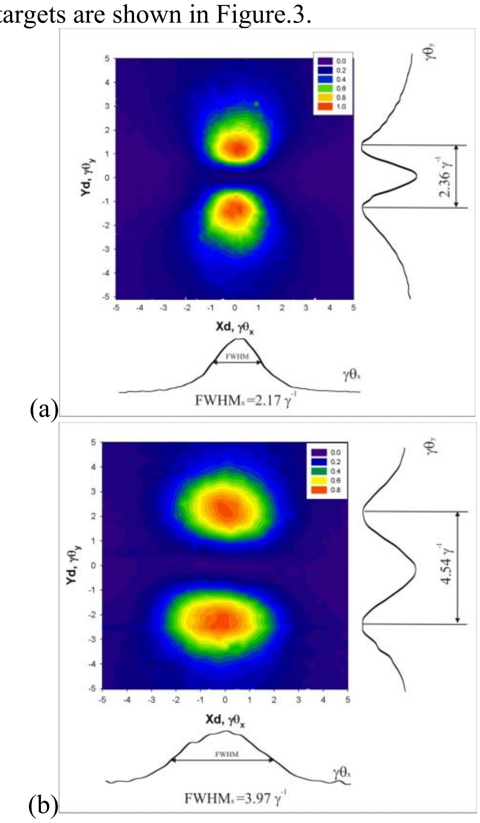

Figure 3. (a) Three-dimensional distribution of the OTR vertical polarization component from the spherical target. (b) – the same from the flat target. Solid lines represent the projections.

Two-dimensional OTR distributions along the vertical (Yd) direction (for Xd=0) are shown in the Figure 4 by the gray circles for the spherical target, and for the flat target – by the open squares. The theoretical predictions for the spherical target are shown in the Figure 4 by a solid line and for the flat target – by a dashed line. The estimations were made for wavelength λ=550 nm.

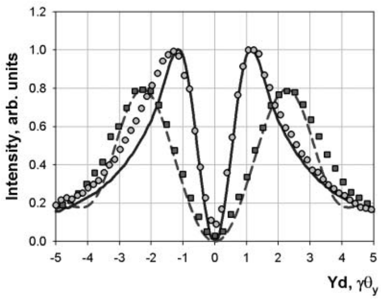

Figure.4. The two-dimensional distributions along Yd direction (for Xd=0) measured from the spherical target (gray circles) and from the flat one (dark gray squares), and calculated distributions: the spherical target – solid line, the flat target – dashed line.

From the Figure.4 one can see that OTR angular distribution from the spherical target is narrower than from the flat one. The interpeak distance of OTR distribution from the spherical target is 2.36 γ^{-1}, and from the flat target – 4.54 γ^{-1}. The angular distribution from the spherical target in the pre-wave zone is very similar to the far-field zone distribution with well-known inter-peak distance of 2 γ^{-1} [7,8].

(a) (b)

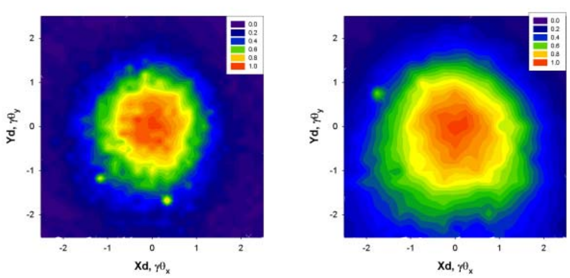

Figure 5. (a) Three-dimensional distribution of the ODR vertical component from the spherical target. (b) – the same from the flat target. Impact-parameter h = 45 μm. Distributions were normalized on maximum

The ODR angular distributions of the vertical polarization component without optical filters from both targets have also been measured. Three-dimensional distributions of the ODR vertical component from the spherical target and from the flat one for impact-parameter h = 45 μm are shown in Figure 5.

The main characteristic of the ODR is the dependence of the distribution width (FWHM) in horizontal direction ($\gamma\theta_x$) vs. impact-parameter [8]. This dependence is shown in Figure 6. The FWHM decreases as the impact parameter increases. The lines represent the theoretical prediction. It is clear that the experiment is in good agreement with the theory.

From the Figure 6 one can see that ODR distribution from the spherical target is narrower than from the flat one. The theoretical predictions and the experimental results are in good agreement. A little disagreement might be explained by the influence of the vertical beam size which was not taken into account in the theoretical model and by the influence of joint action of CCD-detector spectral efficiency and Fresnel reflection coefficients of the target materials.

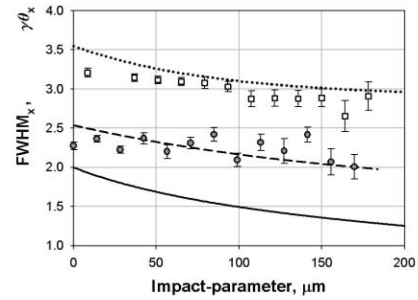

Figure 6. ODR FWHM vs. impact-parameter. Gray circles – the spherical target experiment, open squares – the flat target experiment. Solid line – far-field zone approach, dashed line – spherical target theoretical predictions, dotted line – flat target theoretical predictions. The estimations were made for wavelength λ=550 nm.

CONCLUSION

Finally we can say that during this proof-of-principle experiment the OTR and ODR focusing by the spherical target was clearly observed. The received experimental distributions are in good agreement with the theoretical predictions. One may expect that coherent TR and coherent DR may be focused too. Received results allow to hope that the spherical target application will be widely adopted in different beam diagnostics tools. For instance, using the focusing of CDR by a concave target electro-optic diagnostics becomes noninvasive and more sensitive due to placement of EOC at the minimal possible distance in the extreme pre-wave zone. Moreover it might simplify the performance of the method.

REFERENCES

1. M. Ross, S. Anderson, J. Frisch, et al., SLAC-PUB-9280 (July 2002).
2. P.Karataev, S. Araki, R. Hamatsu et al., PRL, 93, 244802 (2004)
3. A. Winter, et al., in: Proceedings of EPAC 2004, Lucerne, Switzerland, 2004, p.253
4. A.P. Potylitsyn, L.G. Sukhikh, A.S. Kostousov, J. Urakawa, A. Aryshev, S. Boogert, P.V.Karataev, http://rupac2006.inp.nsk.su/ready/mono07.pdf
5. V.A. Verzilov, Phys. Lett. A 273 (2000) 135.
6. A.P. Potylitsyn, R.O. Rezaev, NIMB **252** (2006) 44.
7. P.V. Karataev, Phys. Lett. A **345** (2005) 428-438
8. T.Muto, S. Araki, R. Hamatsu, et al., PRL 90, 10 (2003) 104801.
9. SAD, Strategic Accelerator Design, http://acc-physics.kek.jp/SAD/sad.html
10. P. Karataev, PhD thesis, Tokyo Metropolitan University, 2004
11. P.Karataev, et al., European Part. Accel. Conf., July 5-9, 2004, Lucerne, Switzerland, p. 2643